An Iterative Refinement DSA Image Registration Algorithm Using Structural Image Quality measure

Jiang WANG, Jian Qiu ZHANG
Dept. of E. E., Fudan University, Shanghai 200433, P. R. CHINA
Tel: +86-21-55664226, Fax: +86-21-55664226,
E-mail: wangjiangb@gmail.com; jqzhang@fudan.ac.cn

***Abstract*—This paper proposes a iterative robust algorithm for the registration of digital angiography images. The registration is iteratively refined with the extracted vessel information and the SSIM index is employed as similarity measure. The experimental results show that proposed algorithm yields good global and local registration, and SSIM index outperforms MI as a similarity measure in the DSA image registration.**

***Keywords*-Image registration, digital subtraction angiography, image quality assessment, mutual information**

I. INTRODUCTION

In modern clinical practices, it is a common practice to use digital subtraction angiography (DSA) on X-ray images to visualize blood vessels. The major problem encountered in DSA images is the presence of motion artifacts arising from the misalignment of successive images in the sequence as well as the peristaltic motion of the patients . Therefore, registration is usually performed to the mask and live images prior to subtracting the images.

Image registration is the process of finding the geometrical transformation that aligns the images in such a way that the points in the two images corresponding to the same physical region of the scene being imaged. An overview of image registration is given in [1] in general, in [2] for medical image analysis, and in [3] for DSA image registration. Since the deformation of the X-ray images is highly nonlinear, the feature-based image registration is usually employed. Many efforts have been made to register DSA images with the feature-based image registration technique [4]–[6]. In these technique, correspondences between the pixels of the mask and live images are searched first. Then a certain warping method is applied to the mask image according to the correspondences with respect to the live one. However the non-rigid motion of the tissue inside the human body is complicated and often there are global and local disparities between the mean gray-levels of the live and mask images. Registration of such kind of angiographic images is very difficult, a simple rotation or shift of the misregistered image cannot eliminate the artifacts.

This work was supported by the National Natural Science Foundation of China under Grant 60872058 and the National Key Basic Research Program (NKBRP) of China under Grant 2006CB705700

A novel registration algorithm is proposed here for DSA images, which can be outlined as follows. Firstly, we extract control points by sampling the interest points of live images. Secondly, we use structural similarity (SSIM) index in [7] as the similarity measure to find the correspondence between two images. Thirdly, we perform correction according to this correspondence, by warping the mask image with thin-plate spline. Forthly, the blood vessel is extracted by subtracting the live image with the registered mask image and performing outlier object detection algorithm proposed in [8]. Finally, the coarsely extracted blood vessel is used to help extracting more useful control points for registration in the next iteration.

The rest of the paper is organized as follows, In section II, our algorithm is described in detail. Some experimental results are shown in section III. And section IV concludes this paper.

II. REGISTRATION ALGORITHM

The most significant difference of our algorithm from the traditional algorithms is that our registration results are obtained by iteratively refining the registration with the extracted blood vessel information. Since we are only interested with the regions near the blood vessels, the control points are only extracted from these regions. Moreover, we increase the patch size and decrease the search region size at each iteration to obtain more accurate correspondence information.

A. control points extraction

To explicitly compute the correspondence for each pixel might be desirable but unpractical, due to the expensive computation cost. Therefore, we merely calculate the correspondences for a selected control points. The control points can be selected manually, by taking a regular grid, or by interest point detector. In this paper, we select the control points by performing an interest point detector because interest point can be more robustly matched. An overview of interest point detectors is given in [9]. In this paper, the Harris corner detector [10] is employed to extract control points because of its robustness.

Moreover, since it takes too much computation cost to match all the interest points extracted by the Harris corner detector, we sampling the Harris corners with $m \times m$ slipping windows to ensure only one control point in a window. The larger m is, the smaller the number the control points. In this paper, m is chosen to be 60 at the beginning, and is decreased by 4 at each following iteration.

B. control point correspondence calculation

After extracting the control points, we now search the correspondence points between the live and the mask images. We employ a template-matching based technique to find the correspondences. If a mask image point's local patch has the maximum similarity with the local patch of a control points in the live image, this point is selected as the corresponding control point. That is, for each control point x, y, we are to find x_p, y_p such that:

$$(x_p, y_p) = \arg\max_{x_p, y_p} S(I_l(x, y), I_m(x_p, y_p)l) \tag{1}$$

Where $S(.,.)$ is a similarity measure, I_m and I_l are the local patches in the mask and live image respectively. Since the deformation between the mask and the live image is generally small in our application, we assume that $|x_p - x|$ and $|y - y_p|$ would not exceed n pixels shift for a certain translation. The possible correspondence regions are exhaustively searched so that the correspondence points maximize the similarity measure between the patches in the live and mask image. In this paper, n is chosen to be 30 at the beginning and is decreased by 2 at each following iteration.

The SSIM index measure is utilized here to describe the similarity of the DSA image pairs. The SSIM index is first proposed in [7] to evaluate the image quality. Since the human vision system is strongly specialized in learning about the scene through extracting structural information, it can be expected that the perceived image quality can be well approximated by measuring structural similarity between the images, which is exploited by SSIM to evaluate the image quality. The SSIM of two images x and y is defined as:

$$\begin{aligned} \text{S(x, y) = l(x, y).c(x, y).s(x,y) = } & \left(\frac{2\mu_x\mu_y + C_1}{\mu_x^2 + \mu_y^2 + C_1}\right) \\ & \cdot \left(\frac{2\delta_x\delta_y + C_2}{\delta_x^2 + \delta_y^2 + C_2}\right) \cdot \left(\frac{2\delta_{xy} + C_3}{\delta_x\delta_y + C_3}\right) \end{aligned} \tag{2}$$

where μ_x and μ_y are (respectively) the local sample means of x and y, δ_x and δ_y are (respectively) the local sample standard deviations of x and y, and δ_{xy} is the sample cross correlation of x and y after removing their means. The items C_1, C_2 and C_3 are small positive constant that stabilize each term, so that near-zero sample means, variance, or correlations do not leads to numerical instability .

Recently, the SSIM index is suggested as a similarity measure in [11]. Because it is sensitive to structural distortion while insensitive to nonstructural distortion. This property is desirable because this similarity measure can identify the local structure deformation while ignore some non-structural changes such as intensity changes. Moreover, since image quality measures image similarity that accords with visual perception. Utilizing it as similarity measure can produce results that matches biological perceptual systems. Therefore, we employ SSIM index to find the correspondence.

C. image warping by thin plate spline

The use of thin-plate spline (TPS) interpolation as a point-based elastic registration algorithm for medical images was first proposed by Bookstein [12]. One of the most important attributes of thin-plate spline is its ability to decompose a sparse transformation into a global affine transformation and a local non-affine warping component while minimizing a bending energy based on the second derivative of the spatial mapping. Once the corresponding points are restricted, matching matrixes and mapping parameters can all be achieved.

Given the control points pairs U and V, which are represented as $u_a : a = 1, 2, \ldots, n$ and$v_a, a = 1, 2, \ldots, n$ respectively. Then the energy function of the thin-plate spline can be expressed as:

$$\begin{aligned} E_{TPS(f)} = & \sum_{a=1}^{n} \|u_a - f(v_a)\|^2 + \\ & \lambda \iint \left[\left(\frac{\partial^2 f}{\partial x^2}\right) + 2\left(\frac{\partial^2 f}{\partial x \partial y}\right) + \left(\frac{\partial^2 f}{\partial y^2}\right)\right] dxdy \end{aligned} \tag{3}$$

where f is the mapping function between the point set v_a and u_a. $(1, v_{ax}, v_{ay})$ and $(1, u_{ax}, u_{ay})$ are the homogeneous coordinates of v_a and u_a respectively, and λ is a regularization parameter which adjust the degree of smoothness of the TPS function. Large values of λ limit the range of non-rigidity of the transformation. For any fixed λ, There exists a minimizing function $f(v)$, which can be represented as:

$$f(v) = v.d + \phi(v).w \tag{4}$$

where v is the calculated point sets, d is a 3×3 affine transformation matrix, w is a $n \times 3$ non-affine warping coefficient matrix, $\phi(v)$ is a $1 \times n$ vector decided by TPS kernel. For each point of v, there exists a $\phi_a(v)$, which can be defined as $\phi_a(v) = c\|v - v_a\|^2 log\|v - v_a\|$, where c is a constant.

When the solution of (3) is substituted into (4), the TPS energy function becomes:

$$E_{TPS}(A, W) = \|U - VA - \phi w\|^2 + \lambda trace(W^T \Phi W) \tag{5}$$

where Φ is a $N \times N$ matrix made up by $\phi(v_a)$.

Then, QR factorization can be used to separate the affine and non-affine warping space.

$$V = [Q_1 Q_2] \begin{pmatrix} R \\ 0 \end{pmatrix} \tag{6}$$

where Q_1 and Q_2 are orthonormal matrices. R is upper triangular. The final solution for w and d can be written as

$$w = Q_2(Q_2^T \Phi Q_2 + \lambda I_{N-3})^{-1} Q_2^T U \tag{7}$$

$$d = R^{-1} Q_1^T (U - \Phi w) e35 \tag{8}$$

Then, using the function with the calculated parameters, we apply this warping to each pixel of the mask image to obtain a new registered mask image.

D. outlier object detection

The blood vessel detection is formulated as a outlier detection problem using the algorithm proposed in [8]. However, the lighting condition of our DSA images do not change, therefore, intensity compensation is not performed. The influence of the outlier is defined in an additive outlier image model. Let v_a and u_a denote the observations, and r_a denote the outlier image to be added. The outlier image model is then given by

$$u_a = v_a + r_a + \varepsilon_a, a = 1, \ldots, m \tag{9}$$

where m is the number of pixels of the image, and ε_a is a Gaussian distributed additive noise. If a pixel a is a outlier pixel $r_a \neq 0$, otherwise, the pixel a is a inlier pixel.

In order to find the outlier, the residual $u_a - v_a$ is examined. To make the measure insensitive to the variance δ^2, we consider a scaled residual ρ_a, which is defined by

$$\rho_a = \frac{u_a - v - a}{\delta} \tag{10}$$

where unbiased estimate of δ^2 is obtained by s^2

$$s^2 = \frac{1}{m-2} \sum_{l=1}^{m} u_l - v_l \tag{11}$$

We set a threshold D. The samples that satisfy $|p_a| > D$ are regarded as the possible outliers.

To remove the possible spurious outliers that form small objects or holes in a object, morphological filtering is applied to the possible outlier using a disc structuring element. The applied morphological filtering is composed of opening and then closing [13].

Since only the blood vessels are of interest, only the regions near the blood vessels are displayed. And at the next iteration, only the regions near the blood vessels are registered to refine the registration results.

III. Experimental Results

A. Evaluation of Algorithm on Simulated Data

The algorithm is first applied to simulated images, a live image and its elastically warped versions as the correct image. The control points are selected randomly from the live image, which can be represented as (x_i, y_i), where $i = 1, 2, \ldots, K$ and K is the number of control points. An uncorrelated random shift dx, dy to both x and y dimensions ranging from $-\delta$ to δ is added. A new set of random control points are thus formed, which can be written as $(x_i + dx_i, y_i + dy_i)$. With the generated control points, a new simulated live image is produced by thin-plate spline. The left bottom image in Fig 1 illustrate the direct subtraction of the two images. One can find that a great deal of artifacts exist in figure. Then these two images are registered with mutual information (MI) and SSIM as similarity measure respectively. Fig. 1 illustrate the registration results of a live image using MI and SSIM as similarity measure. It can be observed that image is better registered with SSIM index.

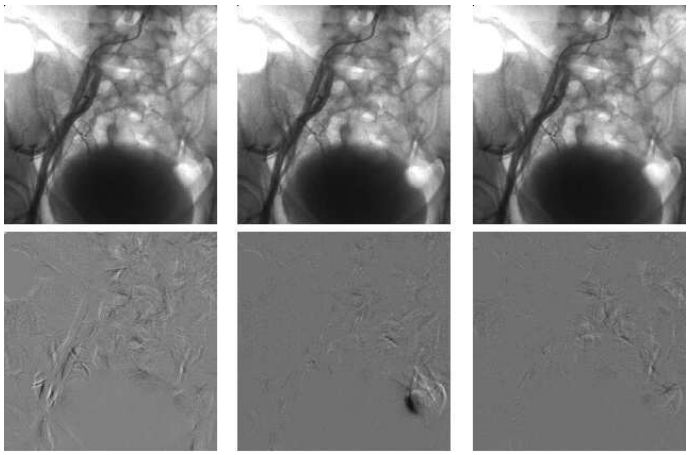

Figure 1. Registration results using different similarity measures. The top row from left to right correspond the original live image, live image registered using MI , and live image registered using SSIM. The bottom row. The bottom row contains the substraction image in the same order of the top row.

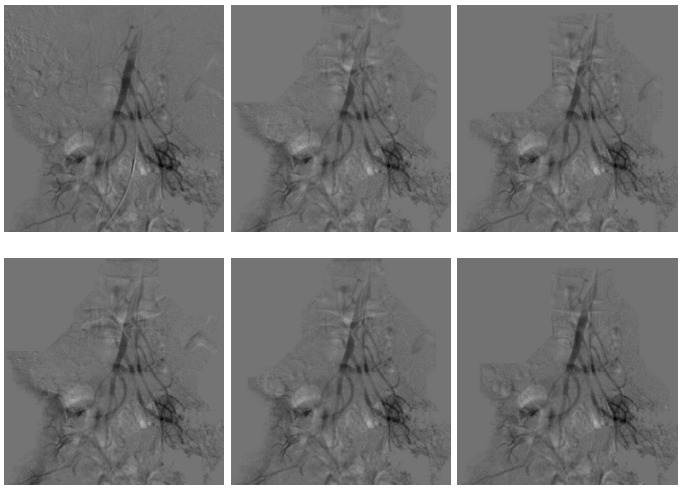

Figure 2. Iterative registration results. (a) is the original subtraction of live image from the mask image showing significant artifacts. (b)-(f) are substraction results from iteration one to iteration five respectively.

Moreover, we evaluate the registration performance by calculating the RMSE between the registered image and

Data sets	No. 1	No. 2	No. 3	No. 4	No. 5	No. 6	No. 7	No. 8
RMSE using SSIM	2.3037	2.4956	2.1117	2.4365	3.1938	3.2432	2.7182	2.5329
RMSE using MI	3.9968	4.3434	3.0851	3.2851	4.8936	4.7780	4.2132	4.3354

Table I
COMPARISON OF REGISTRATION RESULTS FOR DIFFERENT SIMILARITY MEASURES

the correct image. We use eight pairs of DSA images in our experiment. The RMSE values are tabulated in Table I. Obviously, registration using SSIM index performs better than that using MI in terms of RMSE.

B. Experiments on Clinical Cardiac Angiographic Images

In this subsection, the registration algorithm is applied to different clinical angiographic image data sets. The detailed results on one of the data sets, where the registration results of each iteration is illustrated in Fig. 2. Notice that the shown results only show the regions near the blood vessels. It can be observed that the registration accuracy is improved at each iteration. Compared with the direct substraction results before registration, the improvement is obvious.

IV. CONCLUSIONS

In this paper, a iterative robust algorithm for the registration of digital angiography images is proposed. The proposed algorithm iteratively refines the registration with the extracted vessel information and employs the SSIM index as similarity measure. The experimental results show that proposed algorithm yields good global and local registration, and SSIM index outperforms MI as a similarity measure in the DSA image registration.

Further research will focus on the exploit of the deformation prior of the tissues and implement more sophisticated blood vessel detection algorithm.

REFERENCES

[1] B. Zitova and J. Flusser, "Image registration methods: a survey," *Image and vision computing*, vol. 21, no. 11, pp. 977–1000, 2003.

[2] J. B. A. Maintz and M. A. Viergever, "A survey of medical image registration," *Medical image analysis*, vol. 2, no. 1, pp. 1–36, 1998.

[3] E. H. W. Meijering, K. J. Zuiderveld, and M. A. Viergever, "Image registration for digital subtraction angiography," *International Journal of Computer Vision*, vol. 31, no. 2, pp. 227–246, 1999.

[4] J. Yang, Y. Wang, S. Tang, S. Zhou, Y. Liu, and W. Chen, "Multiresolution elastic registration of X-Ray angiography images using Thin-Plate spline," *IEEE Transactions on Nuclear Science*, vol. 54, no. 1 Part 1, pp. 152–166, 2007.

[5] Z. Cao, X. Liu, B. Peng, and Y. S. Moon, "DSA image registration based on multiscale gabor filters and mutual information," in *2005 IEEE International Conference on Information Acquisition*, p. 6.

[6] Y. Bentoutou and N. Taleb, "Automatic extraction of control points for digital subtraction angiography image enhancement," *IEEE Transactions on Nuclear Science*, vol. 52, no. 1 Part 1, pp. 238–246, 2005.

[7] Z. Wang, A. C. Bovik, H. R. Sheikh, and E. P. Simoncelli, "Image quality assessment: From error visibility to structural similarity," *IEEE transactions on image processing*, vol. 13, no. 4, pp. 600–612, 2004.

[8] D. S. Kim and K. Lee, "Block-Coordinate Gauss-Newton optimization and constrained monotone regression for image registration in the presence of outlier objects," *IEEE Transactions on Image Processing*, vol. 17, no. 5, pp. 798–810, 2008.

[9] K. Mikolajczyk, T. Tuytelaars, C. Schmid, A. Zisserman, J. Matas, F. Schaffalitzky, T. Kadir, and L. V. Gool, "A comparison of affine region detectors," *International Journal of Computer Vision*, vol. 65, no. 1, pp. 43–72, 2005.

[10] C. Harris and M. Stephens, "A combined corner and edge detector," in *Alvey vision conference*, 1988, vol. 15, p. 50.

[11] Z. Wang and A. C. Bovik, "Mean squared error: Lot it or leave it? a new look at signal fidelity measures," *IEEE Signal Processing Magazine*, vol. 26, no. 1, pp. 98–117, 2009.

[12] F. L. Bookstein, "Principal warps: Thin-plate splines and the decomposition of deformations," *IEEE Transactions on pattern analysis and machine intelligence*, vol. 11, no. 6, pp. 567–585, 1989.

[13] RCGRE Woods and R. Gonzalez, "Digital image processing," *Prentice Hall*, 2002.